JOURNAL OF SOLID STATE CHEMISTRY 55, 110–115 (1984)

Nature of Th–F Bonding in Crystalline and Glassy States Using EXAFS and XANES

K. J. RAO* AND J. WONG

General Electric Corporate Research and Development, P.O. Box 8, Schenectady, New York 12301

AND M. W. SHAFER

IBM Watson Research Center, Yorktown Heights, New York 10598

Received January 31, 1984; in revised form June 11, 1984

A binary glass of thorium and hafnium tetrafluorides (with dopant concentrations of LaF_3) has been investigated using EXAFS and XANES analysis of the L_{III} edge spectra of thorium. Results of EXAFS analysis indicate that there is no change in the number of nearest neighbors of thorium ions. However, the intensity of the white line in XANES is significantly higher in the glass. This increase in intensity has been explained semiquantitatively in terms of enhanced covalency of Th–F bonding. Since the coordination number of Th^{4+} remains constant in both crystalline and glassy states, covalency enhancement seems to be a general characteristic of glassy state of ionic materials.

1. Introduction

It is generally known (*1*) that the more covalently bonded materials are easy glass formers. In an earlier investigation of chemical shifts (*2*) it was suggested that the extent of covalency is higher compared to their parent crystalline states. We have also reported (*3*) that the white-line intensities of L_{III} and L_{II} edges of Nd^{3+} are quite sensitive to small variations in the nature of the bonding. However, in the case of a NdF_3–BeF_2 glass (*3*) the coordination number of Nd^{3+} was also found to be lower in the glass than in crystalline NdF_3.

ThF_4–HfF_4 glasses (*4*) are unique in that they are formed from isovalent tetrahalides. In such glasses it is conceivable that the local coordinations of cations do not change. If the coordination numbers do not change and still variations in absorption intensities at L-edges occur, it would be possible to consider such variations as incidental to glassy state and hence to the more covalent nature of bonding in the glassy state.

In this study of the Extended X-ray Absorption Fine Structures (EXAFS) and X-ray Absorption Near Edge Structure (XANES) associated with the L_{III} edge of Th^{4+} ions (*5*) (16,300.0 eV) in crystalline ThF_4 and a glass of composition 0.33 ThF_4

* Visiting Research Fellow from Indian Institute of Science, Bangalore, India.

0022-4596/84 $3.00

$\cdot$ 0.6 HfF_4 $\cdot$ 0.07 LaF_3, we have determined the local coordination of Th^{4+} in the glass using the phase parameters (Th–F_4 pairs) determined from the EXAFS analysis of crystalline ThF_4 and have compared the normalized white-line intensities of the L_{III} edge XANES of Th^{4+} in the ThF_4 and the glass. We have found that the coordination number of Th^{4+} remains equal to 8 in the glass also while the absorption intensity is ~12% higher in the glass. We attribute the intensity increase to the presence of electrons in valence 6*d* levels of Th^{4+} which result from an increase of covalency of Th–F bonding. Such repopulation of valence 6*d* levels is shown to affect the matrix element characterizing to L_{III} edge transition through a screening effect in a manner consistent with the observed trend.

2. Experimental

The glasses used in this investigation were prepared by heating the metal oxides in the presence of excess ammonium bifluoride according to the reaction $(Hf,Th)O_{2(s)} + 4NH_4F.HF_{(s)} \rightarrow (HF,Th)F_{4(s)} + 2H_2O_{(g)} + 4NH_4F_{(g)}$ at about 400°C then fusing at 850–900°C to form a glass.

Samples for EXAFS and XANES investigation were prepared by making fine powders (−400 mesh) of the materials with Duco cement and casting the mull into films between glass slides. The procedure is discussed in detail elsewhere (*6*). The concentration of Th^{4+} in each such film is controlled such that it corresponds to about two absorption lengths at the L_{III} edge. Spectra were recorded at CHESS (Cornell High-Energy Synchrotron Source) facility at Cornell with CESR (Cornell Electron Storage Ring) operating at an electron energy of ~5.2 GeV and injection current of ~15 mA. The X-ray beam (C2 spectrometer) was monochromated with a channel-cut Si (220) crystal. Spectra were scanned with the C2 spectrometer at CHESS. The ThL_{III} edge was calibrated using PbL_I edge (*5*) (15,860.8 eV) from Pb metal. Detailed procedures for obtaining normalized XANES are given elsewhere (*7*). The smooth background in the EXAFS region was curve-fitted with a cubic spline using four equal segments and the background in the pre-edge region was determined by a linear regression analysis of the first 10 raw data points. The edge jump, S, was determined as the difference between the extrapolated valves of the post-edge and pre-edge background at $E - E_b = 0$. E_b is the L_{III} edge energy of the Th at 16300 eV. The near-edge spectra was normalized by dividing the intensities by S. The normalized EXAFS, $\chi(k)$ was determined as

$$\chi(k) = \frac{\mu(k) - \mu_0(k)}{S \cdot M(k)}, \qquad (1)$$

where $\mu(k)$ is the observed absorption, $\mu_0(k)$ is the extrapolated post-edge background absorption, and $M(k)$ is the McMaster Correction (*8*). Wave vector k is equal to $(1/\hbar)\sqrt{2m(E - E_b)}$. The $\chi(k)$ was Fourier-transformed and the first peak in the region of 0.70–3.00 Å was inverse Fourier-transformed to isolate the EXAFS originating from the shell of F^- ions.

3. Results and Discussion

EXAFS analysis. The results of EXAFS analysis of crystalline ThF_4 and the glass are presented in Figs. 1 and 2, respectively. Raw spectra are shown in Figs. 1a and 2a while $\chi(k) \cdot k$ are presented in 1b and 2b. The Fourier transforms of $\chi(k)$ (the radial structure function, r.s.f.) are presented in 1c and 2c, respectively, for crystalline ThF_4 and the glass. The k-range of transforms was limited to 9.25 $Å^{-1}$ since the EXAFS signal was very weak and the spectra was noisy beyond 9.25 $Å^{-1}$. The scattering amplitudes of F^- ions are known to be low beyond this region and its neglect would not affect the analysis adversely.

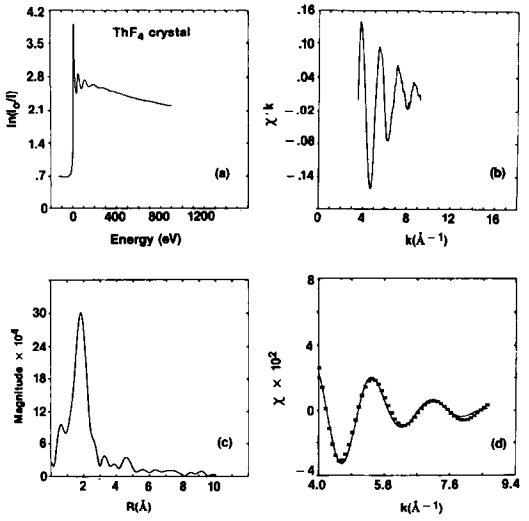

FIG. 1. (a) Room-temperature experimental scan of Th L_{III}-edge XANES and EXAFS in crystalline ThF_4. The energy scale is with respect to the Th L_{III}-edge energy (16,300 eV) taken as zero. (b) Normalized EXAFS as $\chi(k) \cdot k$ versus k. (c) Fourier transform of (b). (d) Inverse transform (line) and simulated EXAFS (points) of the first shell in (c) in the region 0.7 to 3.0 Å.

The inverse Fourier transform, $\chi^F(k)$, generated from the respective first peaks in r.s.f. are shown in Figs. 1d and 2d as solid lines. These were curve fitted to the theoretical EXAFS function (*9*)

$$\chi(k) = -\frac{1}{k}\sum_j A_j \sin[2r_j k + \Phi_j(k)], \quad (2)$$

where

$$A_j = (N_j/r_j^2) f_j(\pi,k) \exp(-2r_j/\lambda) \exp(-2\sigma_j^2 k^2), \quad (3)$$

$\Phi_j(k)$, $f_j(\pi,k)$, and λ are the phase shift, amplitude, and mean free path, respectively, of the scattered electron (scattering parameters) and N_j, r_j, and σ_j are the number of neighbors, distances, and their mean spread, respectively (structural parameters), corresponding to the jth shell of neighbors. The phase shifts are expressed parametrically using the expression

$$\Phi(k) = p_0 + p_1 k + p_2 k^2 + p_3/k^3. \quad (4)$$

As pointed out earlier, EXAFS of crystalline ThF_4 was analyzed in order to obtain $\Phi(k)$ for the Th–F pairs. ThF_4 is isostructural with ZrF_4^{10} and Th^{4+} is surrounded by $8F^-$ neighbors, but the Th–F distances are not known exactly. We estimated the distances using known range of Zr–F distances in ZrF_4 and the difference in ionic radii (*11*) of Th^{4+} and Zr^{4+} ($r_{Th}^{4+} = 1.20$; $r_{Zr}^{4+} = 0.98$). The two extreme Th–F distances were thus taken to be 1.83 and 1.98 Å. Scattering amplitudes for F^- ions were taken from tabulations of Teo and Lee (*12*).

EXAFS curve fitting was performed using P's and σ as adjustable parameters. Fitting was found unsatisfactory when a single average Th–F distance was used. The fitting was unsatisfactory even when the two extreme Th–F distances were used in two fluorine subshells of the $4F^-$ ions each. A good fit could however be obtained using three subshells of the F^- ions with 3, 3, and 2 F^- ions at 1.83, 1.91, and 1.98 Å, respectively. The phase parameters and σ^2 values

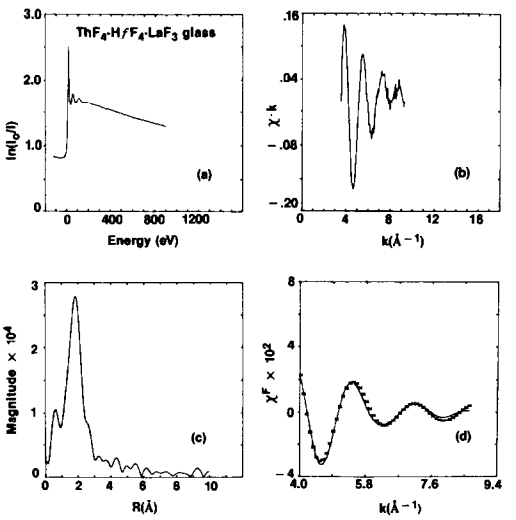

FIG. 2. (a) Room-temperature experimental scan of Th L_{III}-edge XANES and EXAFS in 0.33 ThF_4 · 0.6 HfF_4 · 0.07 LaF_3 glass. (b) Normalized EXAFS as $\chi(k)$ · k versus k. (c) Fourier transform of (b). (d) Inverse transform (line) and simulated EXAFS (points) of the first shell in (c) in the region 0.7 to 3.0 Å.

so determined for the three subshells are given in Table I. Corresponding fit is shown in Fig. 1d as crosses. It may be noted from Table I that the phase parameters for the three subshells are satisfactorily close. The structure of the glass was analyzed in the same k region using the phase shift parameters of Table I. N_j, r_j, and σ_j were treated as adjustable parameters in the EXAFS fitting. A good fit (crosses in Fig. 2d) could be obtained in the case of glass also only with the use of three subshells of F^- ions. The structural parameters so obtained are given in Table II.

It may be seen that the total number of neighbors in the three subshells of Th^{4+} in glass is equal to 8.13 which is equal to the coordination number of Th^{4+} in crystalline ThF_4 (=8) within 1.5%. We may therefore infer that the near-neighbor coordination number of Th^{4+} remains unaltered upon glass formation. The Th–F distances in the glass obtained in the fitting are also very nearly equal (within 0.01 Å) to those in crystalline ThF_4 shown in Table I. Of interest also are the lower σ_j^2 values of the two innermost subshells with respect to those of the crystal. This may be reflective of a covalency effect due to glass formation discussed below.

XANES intensities and covalency. The normalized XANES spectra of the L_{III} edge of Th^{4+} in crystalline ThF_4 and the glass are shown in Fig. 3. The white-line intensity (measured at the peak) is about 12% higher in the glass than in crystalline ThF_4. In order to understand this variation, we may note that the absorption coefficients are governed by the values of the transition dipole matrix element in the equation (*13*)

$$\mu = \frac{4\pi^2}{n}\frac{e^2}{\hbar c}\hbar\omega \sum_{i,j} |M'_{ij}|^2 \delta(E_i - E_j - \hbar\omega). \quad (5)$$

In Eq. (5), $M'_{ij} = \langle j|r_A|i\rangle$ is the dipole matrix element connecting the two states $\langle j|$ and $|i\rangle$; δ is the Kronecker data; E_i and E_j are the initial and final state energies; n is the refractive index and c is the velocity of light. For the L_{III} edge transition in Th^{4+} the initial and final states correspond to the core $2p$ and valence $6d$ levels. In the one-elec-

TABLE I

PHASE PARAMETERS FOR Th–F SCATTERING PAIRS FROM THE EXAFS OF L_{III} EDGE OF Th^{4+} IN CRYSTALLINE ThF_4

N	r (Å)	σ^2 (Å²)	P_0	P_1	P_2	P_3
3.0	1.830	0.01103	4.1263	−1.2134	0.0293	−29.42
3.0	1.910	0.00785	4.3893	−1.1760	0.0329	26.25
2.0	1.980	0.00026	4.7721	−1.1367	0.0356	96.23

Note. Standard deviation in curve fitting was found to be 6.6% of the maximum amplitude of $\chi(k)$.

TABLE II

STRUCTURAL PARAMETERS OF 0.33 ThF_4 · 0.60 HfF_4 · 0.07 LaF_3 GLASS FROM EXAFS ANALYSIS OF L_{III} EDGE

N (Å)	r (Å)	σ^2 (Å²)	Standard deviation of EXAFS fit
2.89	1.83	0.0092	
3.17	1.92	0.0065	7%
2.07	1.99	0.0005	

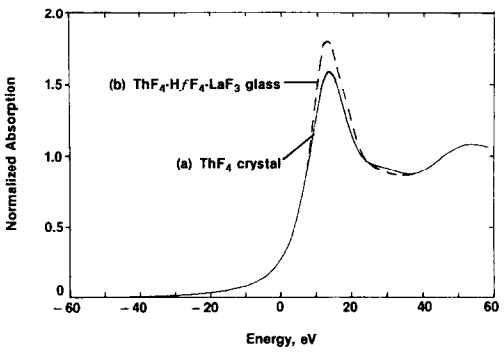

FIG. 3. Normalized Th L_{III}-edge XANES in (a) crystalline ThF_4 and (b) 0.33 ThF_4 · 0.6 HfF_4 · 0.07 LaF_3 glass.

tron approximation, it has been shown that

$$M'_{ij} = \int_0^\infty U_{n,l}(r) \cdot r \cdot U_{n',l\pm1}\, dr, \qquad (6)$$

where $U_{n,l}$ and $U_{n',l\pm1}$ are the initial and final state wave functions. Assuming the same density of empty $6d$ states the ratio of the absorption intensities (μ_g/μ_c), are the absorption coefficients of glass and crystal respectively, is given by

$$\frac{\mu_g}{\mu_c} = \frac{|M'_{i,j}(\text{glass})|^2}{|M'_{i,j}(\text{crystal})|^2}. \qquad (7)$$

We may therefore investigate the effect of covalency using Eqs. (6) and (7). An increase of covalency in the glass is equivalent to a reverse transfer of a certain fraction of electrons from F^- ions to the central Th^{4+} ion. These electrons repopulate the now-shared $6d$ valence shell of Th^{4+}. As a direct consequence of this repopulation of $6d$ levels, the nuclear potential experienced by the $6d$ levels is additionally screened by such electrons. Hence, the final states $|j\rangle$ in $M'_{i,j}$ are additionally screened as a consequence of increased covalency. Let us assume that ν electrons are back-donated by F^- ions, then the fractional covalency is $\nu/8$ or percentage covalency is $(100\ \nu/8)$. The screening effect of electrons can be estimated by the use of Slater orbitals (*14*) in Eq. (6). Slater orbitals are of the form $\Psi_n = r^{n^*-1} \exp[-(z - s)r/n^*]$, where n^* is the effective quantum number and s is the Slater screening constant. The $2p$ electron (initial state) in Th^{4+} experiences shielding due to seven other $2s$ and $2p$ electrons as well as two $1s$ electrons. The $6d$ electrons (final state) of Th^{4+} experiences shielding due to all the electrons (Slater-grouped electronic structure of Th^{4+} is $1s^2$; $2s^2$, $2p^6$; $3s^2$, $3p^6$; $3d^{10}$; $4s^2$, $4p^6$; $4d^{10}$; $4f^{14}$; $5s^2$, $5p^6$; $5d^{10}$; $5f^0$; $6s^2$, $6p^6$; $6d^{10}$; $6f^0$; $7s^0$).

Thus the value of s in the Slater orbital expression for $2p$ electrons is 4.15 and for the $6d$ electrons is 86. The wave functions, $U_{2,1}(r)$ and $U_{6,2}(r)$ become $r \exp[-(90 - 4.15)r/2]$ and $r^{3.2} \exp[-(90 - 86)r/4.2]$, respectively, for Th^{4+} in crystalline ThF_4 assuming that the bonding in ThF_4 is completely ionic. In the case of glass, $U_{6,2}(r)$ becomes, $r^{3.2} \exp[-(90 - 86 - 0.35\nu)r/4.2]$. Using these wave functions in Eq. (7), we have

$$\frac{\mu_g}{\mu_c} = \frac{\left|\int_0^\infty r^{5.2} e^{-K_g r} \cdot dr\right|^2}{\left|\int_0^\infty r^{5.2} e^{-K_c r} \cdot dr\right|^2}. \qquad (8)$$

Using standard methods of integration, we have

$$\frac{\mu_g}{\mu_c} = \frac{|\Gamma(6.2)/K_g^{6.2}|^2}{|\Gamma(6.2)/K_c^{6.2}|^2} = \left(\frac{K_c}{K_g}\right)^{12.4}. \qquad (9)$$

In Eqs. (8) and (9), $K_g = (4 - 0.35\nu)/4.2 + 85.85/2 = 43.8774 - 0.083\nu$ and $K_c = 43.8774$. Hence

$$\frac{\mu_g}{\mu_c} = \left[\frac{43.8774}{43.8774 - 0.083\nu}\right]^{12.4} \sim 1 + 0.023\nu. \qquad (10)$$

Equation (10), therefore clearly suggests that $\mu_g > \mu_c$ for any positive value of ν or any increase in covalency of bonding. In order that $\mu_g/\mu_c = 1.12$, as observed experimentally, it requires that $\nu = 5.2$ which in turn amounts to 65% covalency. Such a value, we feel, is perhaps very high. However, the quantitative discrepancy is likely to originate from the fact that node-free Slater orbitals are only very approximate. Further, we are not at all clear of the ways in which the relativistic nature of the $2p$ wave functions in Th^{4+} affect the above considerations.

The results discussed above suggest therefore, that even when the nearest neighbor coordination number of the cation (Th^{4+}) does not change, the covalency of bonding to anions (F^- ions) increases in the glassy state. The results also imply that the increase in covalency is a concomitant effect of positional disordering in ionic materials.

Acknowledgments

K. J. Rao would like to thank G. E. Corporate Research and Development for the visiting fellowship.

References

1. L. D. PYE, H. J. STEVENS, AND W. C. LACOURSE (Eds.), *in* "Introduction to Glass Science," Plenum, New York (1972).
2. C. N. R. RAO, P. R. SARODE, R. PARTHASARATHY, AND K. J. RAO, *Philos. Mag.* **41,** 581 (1980).
3. K. J. RAO, J. WONG, AND M. J. WEBER, *J. Chem. Phys.* **78,** 6228 (1983).
4. M. G. DREXHAGE, C. T. MOYNIHAN, AND M. SALCH, *Mater. Res. Bull.* **15,** 213 (1980).
5. J. A. BEARDEN AND A. F. BURR, *Rev. Mod. Phys.* **39,** 125 (1967).
6. K. J. RAO, J. WONG, AND B. G. RAO, *Phys. Chem. Glasses,* in press.
7. K. J. RAO AND J. WONG, submitted for publication.
8. W. H. MCMASTER, N. NERR DEL GRANDE, J. H. HALLET, AND H. HUBBELL, Lawrence Radiation Laboratory, University of Calif. Livermore, VCRL-50174 Sec.II Rev. 1 (1969).
9. J. WONG, *in* "Topics in Applied Physics" (H. J. Güntherodt and H. Beck, Eds.), Vol. 46, chap. 4, Springer, Berlin (1980).
10. R. W. G. WYCKOFF, "Crystal Structures," Interscience, New York (1963).
11. B. K. VAINSHTEIN, "Modern Crystallography," Springer-Verlag, New York (1980).
12. B. K. TEO AND P. A. LEE, *J. Amer. Chem. Soc.* **101,** 2815 (1979).
13. F. C. BROWN, *in* "Synchrotron Radiation Research" (H. Winick and S. Domiach, Eds.), Plenum, New York (1980).
14. J. C. SLATER, *Phys. Rev.* **36,** 57 (1930).